

# Planar and nonplanar nucleus-acoustic solitary waves in thermally degenerate multi-nucleus plasma systems

A. A. Mamun\* and J. Akter

*Department of Physics, Jahangirnagar University, Savar, Dhaka-1342, Bangladesh*

(Dated: September 8, 2020)

The novel thermally degenerate plasma model (based on a system containing relativistically and thermally degenerate inertial-less electron species, non-relativistically and thermally degenerate inertial light nucleus species, and stationary heavy nucleus species) is considered. The basic features of planar and nonplanar solitary structures associated with the thermally degenerate pressure driven nucleus-acoustic waves propagating in such a thermally degenerate plasma system has been investigated. The reductive perturbation method, which is valid for small amplitude solitary waves, is used. It is found that the effects of nonplanar cylindrical and spherical geometries, non and ultra-relativistically degenerate electron species, thermal and degenerate pressures of electron and light nucleus species, and number densities of light and heavy nucleus species significantly modify the basic features (viz. speed, amplitude, and width) of the solitary potential structures associated with thermally degenerate pressure driven nucleus-acoustic waves. The degenerate plasma model under consideration is so general and realistic that it is applicable not only in astrophysical compact objects like hot white dwarfs, but also in space plasma systems like mesospheres containing positively charged heavy particles in addition to electron and ion plasma species.

PACS numbers: 52.35.Sb; 52.35.Mw; 52.35.Dm

## I. INTRODUCTION

The degenerate plasmas are defined as plasmas of so high density that the degenerate pressure (generated due to Heisenberg's uncertainty principle with infinitesimally small uncertainty in position and infinitely large uncertainty in momenta of degenerate plasma species) cannot be neglected in any way [1–10]. They usually contain degenerate electron species [1–10], inertial light nucleus species (viz.  $^1\text{H}$  [1–4] or  $^4\text{He}$  [5–7] or  $^{12}\text{C}$  [5–7]) species, and heavy nucleus species (viz.  $^{56}\text{Fe}$  [11] or  $^{85}\text{Rb}$  [12] or  $^{96}\text{Mo}$  [12]). The degenerate pressure  $\mathcal{P}_{dj}$  exerted by the degenerate plasma species  $j$  (where  $j = e$  for the electron species and  $j = l$  for the light nucleus species) is [3–9]

$$\mathcal{P}_{dj} = \mathcal{K}_j N_j^{\gamma_j}, \quad (1)$$

where  $N_j$  is the number density of the plasma species  $j$ , and  $\gamma_j$  and  $\mathcal{K}_j$  are

$$\gamma_j = \frac{5}{3}, \quad \mathcal{K}_j \simeq \frac{3\pi\hbar^2}{5m_j} \quad (2)$$

for the non-relativistic limit [4–9], and

$$\gamma_j = \frac{4}{3}, \quad \mathcal{K}_j \simeq \frac{3}{4}\hbar c, \quad (3)$$

for the ultra-relativistic limit [4–9], where  $m_j$  is the mass of the plasma species  $j$ ,  $\hbar$  is the reduced Plank constant, and  $c$  is the speed of light in vacuum.

The concept of the ion-acoustic waves [13, 14] leads Mamun [15] to introduce the electron degenerate energy  $E_{e0} = \mathcal{K}_e N_{e0}^{\gamma_e - 1}$  along with the corresponding wave speed  $C_l = (E_{e0}/m_l)^{1/2}$  and wave length-scale  $L_q (= C_l/\omega_{pl})$  [where  $\omega_{pl} = (4\pi N_{l0} Z_l^2 e^2/m_l)^{1/2}$ ,  $Z_l$  being the charge state of the light nucleus species,  $N_{e0}$  ( $N_{l0}$ ) being the number density of the electron (light nucleus) species at equilibrium]. We note that  $E_{e0}$ ,  $C_l$  and  $L_q$  are associated with the equilibrium electron degenerate pressure, and that  $N_{e0} = Z_l N_{l0} + Z_h N_{h0}$  at equilibrium, where  $N_{h0}$  ( $Z_h$ ) is the number density (charge state) of the heavy nucleus species. Mamun [15] has then predicted the degenerate pressure driven (DPD) nucleus-acoustic (NA) waves in degenerate plasma system containing cold non or ultra-relativistically degenerate electron species [2–4], non-degenerate light nucleus species (viz.  $^1\text{H}$  [2–4], or  $^4\text{He}$  [6] or  $^{12}\text{C}$  [7], and stationary heavy nucleus species (viz.  $^{56}\text{Fe}$  [11] or  $^{85}\text{Rb}$  [12] or  $^{96}\text{Mo}$  [12]). The linear dispersion relation for the DPD NA waves [15] is

$$\omega = \sqrt{\frac{\gamma_e}{1+\mu}} \frac{k C_l}{\sqrt{1 + \frac{\gamma_e}{1+\mu} k^2 L_q^2}}, \quad (4)$$

where  $\mu = Z_h N_{h0}/Z_l N_{l0}$ . The linear dispersion relation (4) can be interpreted as follows:

- The DPD NA waves are driven by the electron degenerate pressure and the DPD NA waves exist in any degenerate plasma system at absolute zero temperature, for which the DPD NA waves are completely different from the ion-acoustic waves [13, 14].
- The dispersion relation (4) for the long-wavelength

\*Also at Wazed Miah Science Research Centre, Jahangirnagar University, Savar, Dhaka-1342, Bangladesh.

DPD NA waves ( $kL_q \ll 1$ ) is given by

$$\omega = \sqrt{\frac{\gamma_e}{1+\mu}} kC_l. \quad (5)$$

- The dispersion relation (5) for  $\mu = 0$  becomes

$$\omega = \sqrt{\gamma_e} kC_l, \quad (6)$$

which means that in DPD NA waves, the light nucleus mass density (electron degenerate pressure) provides the inertia (restoring force).

- The phase speed ( $\omega/k$ ) of the long-wavelength DPD NA waves decreases with the rise of the value of  $\mu$ , i.e. with the number density ( $N_{h0}$ ), and charge state ( $Z_h$ ) of the stationary heavy nucleus species for fixed light nucleus number density ( $N_{l0}$ ).
- The length and time scales of the DPD NA waves [15] are far different from those of the ion-acoustic waves, since their restoring forces and the mediums of their propagation are completely different.

Recently, a number of theoretical investigations [16–25] have been made on the nonlinear propagation of the NA waves in degenerate plasma systems. Mamun *et al.* [16, 17] considered the strongly [16] and weakly [17] coupled heavy nucleus fluid, and studied the small amplitude heavy nucleus-acoustic shock [16] and solitary [17] waves in an absolutely cold degenerate electron-light nucleus plasma system. These shock and solitary waves [16, 17] are associated with the dynamics of the heavy nucleus species, but not with that of the light nucleus species. Zaman [18, 19] have examined the effects of nonplanar geometry on the NA shock [18] and solitary [19] waves propagating in absolutely cold degenerate electron-nucleus plasma systems. On the hand, Jannat & Mamun [20, 21] considered an absolutely cold degenerate plasma system containing cold degenerate electron species, cold dissipative [20] and non-dissipative [21] light nucleus species, and studied the effects of the stationary heavy nucleus species on the NA shock [20] and solitary [21] waves. Sultana & Schlickeiser [22] considered an absolutely cold multi-nucleus degenerate plasma with relativistically degenerate electron species to study the arbitrary amplitude NA solitons in an absolutely cold degenerate quantum plasma system. Sultana *et al.* [23] have also investigated the modulated heavy nucleus-acoustic waves and associated rogue waves in the same quantum plasma system. Chowdhury *et al.* [24] have studied the nucleus-acoustic envelope solitons and their modulational instability in an absolutely cold degenerate plasma system. Das & Karmakar [25] have studied the nonlinear propagation of the heavy nucleus-acoustic waves associated with the dynamics of cold heavy nucleus species. We note that in heavy nucleus-acoustic waves, the inertia is provided by the mass density of heavy nucleus species, but not of light nucleus species, and the length and time scales of heavy nucleus species are far different from that

of the NA waves, which are associated with the dynamics of light nucleus species.

The works [16–25] pinpointed above are valid only for absolutely cold degenerate plasma species, but are not valid for the thermally degenerate plasma species, particularly for hot white dwarfs [26–30]. To overcome the limitations of the works, we consider a thermally degenerate plasma (TDP). The TDP species  $j$  are governed by the thermally degenerate pressure [defined as the sum of the degenerate pressure ( $\mathcal{P}_{dj}$ ) and thermal pressure ( $\mathcal{P}_{tj}$ )] of the plasma species  $j$ . The thermal pressure  $\mathcal{P}_{tj}$  of the plasma species  $j$  can be expressed as

$$\mathcal{P}_{tj} = N_j k_B T_j, \quad (7)$$

where  $T_j$  is the thermal temperature of TDP species  $j$ , and  $k_B$  is the Boltzmann constant.

Therefore, in our present work, we consider this novel TDP system containing thermally degenerate electron and light nucleus species, and low dense stationary heavy nucleus species, and investigate small amplitude thermally degenerate pressure driven (TDPD) NA solitary waves (SWs) by the reductive perturbation method [31–33] for one dimensional (1D) planar as well as nonplanar cylindrical and spherical geometries. The novel TDP model under our present consideration is so general that it is applicable in astrophysical compact objects like hot white dwarfs [26–30] as well as in many space environments like mesospheres containing heavy positively charged particles (as dust species) in addition to isothermal electron and inertial ion plasma species [34–36].

The manuscript is structured as follows. The novel TDP model is illustrated in Sec. II. The modified Korteweg-de-Vries (MK-dV) equation is derived by using the reductive perturbation method, and the basic features of the small amplitude TDPD NA solitary waves are investigated by solving the MK-dV equation analytically for 1D planar geometry, and numerically for nonplanar cylindrical and spherical geometries in Sec. III. The novel TDP model under consideration, results obtained from this investigation, and some important applications are briefly discussed in Sec. IV.

## II. TDP MODEL EQUATIONS

We consider the novel TDP system containing thermally degenerate electron and light nucleus species, and stationary heavy nucleus species. We also consider the nonlinear propagation of TDPD NA waves in this TDP system. The dynamics of the thermally degenerate electron species is described by the balance between the electrostatic pressure and thermally degenerate electron pressure, i.e.

$$N_e e \frac{\partial \Phi}{\partial R} = \frac{\partial}{\partial R} (\mathcal{P}_{de} + \mathcal{P}_{te}), \quad (8)$$

where  $\Phi$  is the TDPD NA wave electrostatic potential and  $R$  is the space variable. Now, substituting  $\mathcal{P}_{de}$  and

$P_{te}$  [which are obtained from (1) and (7) for the electron species, respectively], we obtain

$$n_e = \left(1 + \frac{\gamma_e - 1}{\gamma_e} \phi\right)^{\frac{1}{\gamma_e - 1}},$$

$$\simeq \left(\frac{1}{\gamma_e}\right) \phi + \left(\frac{\gamma'_e}{2! \gamma_e^2}\right) \phi^2 + \left(\frac{\gamma'_e \gamma''_e}{3! \gamma_e^3}\right) \phi^3 \dots, \quad (9)$$

where  $\gamma'_e = 2 - \gamma_e$ ,  $\gamma''_e = 3 - 2\gamma_e$ ,  $n_e = N_e/N_{e0}$  and  $\phi = e\Phi/\mathcal{E}_{e0}$  with  $\mathcal{E}_{e0} = E_0 + k_B T_e$ . It is obvious that for the cold degenerate electron species,  $T_e = 0$  and  $\mathcal{E}_{e0} = E_0 = \mathcal{K}_e N_{e0}^{\gamma_e - 1}$ , which mean that  $\phi = e\Phi/\mathcal{E}_{e0} = e\Phi/E_0$ . On the other hand, for the non-degenerate thermal electron species,  $E_0 = 0$  and  $\mathcal{E}_{e0} = k_B T_e$ , which indicate that  $\phi = e\Phi/k_B T_e$ . We note that  $\gamma_e = 1$  reduces the expansion form of (9) to  $n_e = \exp(\phi)$ . Thus, (9) is valid for arbitrary value of  $\gamma_e$ , and is, thus, valid for  $\gamma_e = 1$  (Boltzmann distributed isothermal electron species),  $\gamma_e = 5/3$  (non-relativistically thermally degenerate electron species), and  $\gamma_e = 4/3$  (ultra-relativistically thermally degenerate electron species).

The nonlinear dynamics of the TDPD NA waves in such a new TDP system in planar or nonplanar geometry is governed by

$$\frac{\partial n_l}{\partial t} + \frac{1}{r^\nu} \frac{\partial}{\partial r} (r^\nu n_l u_l) = 0, \quad (10)$$

$$\frac{\partial u_l}{\partial t} + u_l \frac{\partial u_l}{\partial r} = -\frac{\partial \phi}{\partial r} - \frac{5}{2} \beta \frac{\partial n_l^{\frac{3}{2}}}{\partial r} - \frac{\sigma_l}{n_l} \frac{\partial n_l}{\partial r}, \quad (11)$$

$$\frac{1}{r^\nu} \frac{\partial}{\partial r} \left( r^\nu \frac{\partial \phi}{\partial r} \right) = (1 + \mu) n_e - n_l - \mu, \quad (12)$$

where  $\nu = 0$  for 1D planar geometry and  $\nu = 1$  (2) for a nonplanar cylindrical (spherical) geometry;  $n_e$  is given by (9);  $n_l$  is the light nucleus number density normalized by  $N_{l0}$ ;  $u_l$  is the light nucleus fluid speed normalized by  $C_q$  [ $= (\mathcal{E}_{e0}/m_l)^{1/2}$ ];  $r = R/\lambda_q$  with  $\lambda_q = C_q/\omega_{pl}$ ;  $t$  is the time variable normalized by  $\omega_{pl}^{-1}$ ;  $\sigma_l = k_B T_l/Z_l \mathcal{E}_{e0}$ , and  $\beta = (m_e/Z_l m_l)(n_{l0}/n_{e0})^{2/3}$ .

The normalized basic equations (9)–(12) in 1D planar or cylindrical or spherical geometries (depending on value of  $\nu$ ) can be interpreted as follows:

- The equation (9) represents the expression for thermally degenerate inertia-less electron number density, which is valid for the arbitrary value of  $\gamma_e$ .
- The equation (10) represents the continuity equation for the thermally degenerate light nucleus species, where the effects of the source and sink terms are neglected in our present investigation.
- The equation (11) represents the momentum balance equation for thermally degenerate light nucleus species, and the 2nd (3rd) term on the right hand side of (10) is due to the effect of non-relativistically degenerate (isothermal) light nucleus species.

- The equation (12) is Poisson's equation for the DPD NA wave potential, which closes (9)–(11), and the parameter  $\mu$  in (12) is due to the assumption of stationary heavy nucleus species, which is valid since the heavy nucleus plasma frequency is much less than the DPD NA wave frequency because of the heavy mass and low number density of this heavy nucleus species.

It is important to mention here that the gravitational force acting in thermally degenerate electron and light nucleus species, which is inherently very small compared to the other forces under consideration, is neglected for this investigation. We also note that that  $\nu$  arises due to the effects of nonplanar cylindrical ( $\nu = 1$ ) and spherical ( $\nu = 2$ ) geometries.

### III. TDPD NA SOLITARY WAVES

To study the planar and nonplanar DPD-NA solitary waves by the reductive perturbation method [31], we stretch the independent  $x$  and  $t$  as [32, 33]

$$\xi = -\epsilon^{\frac{1}{2}}(r + \mathcal{M}t), \quad (13)$$

$$\tau = \epsilon^{\frac{3}{2}}t, \quad (14)$$

and expand the dependent variables ( $n_l$ ,  $u_l$  and  $\phi$ ) as [31]

$$n_l = 1 + \epsilon n_l^{(1)} + \epsilon^2 n_l^{(2)} + \dots, \quad (15)$$

$$u_l = 0 + \epsilon u_l^{(1)} + \epsilon^2 u_l^{(2)} + \dots, \quad (16)$$

$$\phi = 0 + \epsilon \phi^{(1)} + \epsilon^2 \phi^{(2)} + \dots, \quad (17)$$

where  $\mathcal{M}$  is the phase speed (normalized by  $C_q$ ) of the DPD-NA waves (i.e.  $\mathcal{M} = \omega/kC_q$ ), and  $\epsilon$  is the stretching or expansion parameter with a value satisfying  $0 < \epsilon < 1$ .

Now, using (13)–(17) in (9)–(12), and taking the coefficients of  $\epsilon^{3/2}$  from (10) and (11), and the coefficients of  $\epsilon$  from (12), we obtain

$$n_l^{(1)} = \frac{1}{\mathcal{M}^2 - \beta_\sigma} \phi^{(1)}, \quad (18)$$

$$u_l^{(1)} = \frac{\mathcal{M}}{\mathcal{M}^2 - \beta_\sigma} \phi^{(1)}, \quad (19)$$

$$\mathcal{M} = \left[ \frac{\gamma_e + (1 + \mu)\beta_\sigma}{1 + \mu} \right]^{\frac{1}{2}}, \quad (20)$$

where  $\beta_\sigma = \sigma_l + 5\beta/3$ . We note that (20) represents the linear dispersion relation for the TDPD NA waves. This linear dispersion relation can be written in dimensional form as

$$\omega = kC_q \sqrt{\frac{\gamma_e + (1 + \mu)\beta_\sigma}{1 + \mu}}. \quad (21)$$

It is obvious that for non-degenerate cold light nucleus species,  $\beta = 0$ ,  $\sigma_l = 0$ ,  $C_q = C_l$ , and the dispersion

relation (21) is identical to (5). This means that the linearized equations (18)–(20), which are derived by using the 1st order approximation, are valid for the long wavelength TDPD NA waves.

Similarly, using (13)–(17) in (9)–(12), and taking the coefficients of  $\epsilon^{5/2}$  from (10) and (11), and the coefficient of  $\epsilon^2$  from (12), we obtain

$$\frac{\partial n_l^{(1)}}{\partial \tau} - \frac{\partial}{\partial \xi} \left[ \mathcal{M} n_l^{(2)} + u_l^{(2)} + n_l^{(1)} u_l^{(1)} \right] - \frac{\nu u_l^{(1)}}{\tau \mathcal{M}} = 0, \quad (22)$$

$$\begin{aligned} \frac{\partial u_l^{(1)}}{\partial \tau} - \mathcal{M} \frac{\partial u_l^{(2)}}{\partial \xi} - u_l^{(1)} \frac{\partial u_l^{(1)}}{\partial \xi} &= \frac{\partial \phi^{(2)}}{\partial \xi} + \frac{5}{3} \beta \frac{\partial n_l^{(2)}}{\partial \xi} \\ &+ \frac{1}{2} \left( \sigma_l - \frac{5}{9} \beta \right) \frac{\partial}{\partial \xi} \left[ n_l^{(1)} \right]^2, \end{aligned} \quad (23)$$

$$\frac{\partial^2 \phi^{(1)}}{\partial \xi^2} = \left( \frac{1 + \mu}{\gamma_e} \right) \phi^{(2)} + \frac{(1 + \mu) \gamma_e'}{2 \gamma_e^2} \left[ \phi^{(1)} \right]^2 - n_l^{(2)}, \quad (24)$$

where  $\beta'_\sigma = (\sigma_l - 5\beta/9)/2$ . Using (18)–(24), we eliminate  $\phi^{(2)}$ ,  $u_l^{(2)}$  and  $n_l^{(2)}$  to obtain

$$\frac{\partial \phi^{(1)}}{\partial \tau} + \frac{\nu}{2\tau} \phi^{(1)} + \mathcal{A} \phi^{(1)} \frac{\partial \phi^{(1)}}{\partial \xi} + \mathcal{B} \frac{\partial^3 \phi^{(1)}}{\partial \xi^3} = 0, \quad (25)$$

where  $\mathcal{A}$  and  $\mathcal{B}$  are nonlinear and dispersion coefficients, respectively, and are given by

$$\mathcal{A} = \mathcal{B} \left( \frac{\mu_1}{\gamma_e} \right)^2 \left[ 3 + 2 \frac{\mu_1}{\gamma_e} \left( \sigma_l + \frac{20}{9} \beta \right) + \frac{\gamma_e'}{\mu_1} \right], \quad (26)$$

$$\mathcal{B} = \frac{\gamma_e^2}{2 \mu_1^{\frac{3}{2}} \sqrt{\gamma_e + \mu_1 \beta_\sigma}}, \quad (27)$$

where  $\mu_1 = 1 + \mu$ . We note that (25) is the MK-dV equation with the nonlinear coefficient  $\mathcal{A}$  defined by (26), and the dispersion coefficient  $\mathcal{B}$  defined by (27), and that  $\mathcal{A} > 0$  and  $\mathcal{B} > 0$  for all possible values of  $\gamma_e$ ,  $\mu$ ,  $\sigma_l$ , and  $\beta$ . To avoid any confusion, we also note that  $1 \geq \gamma_e < 2$  since  $\gamma_e = 1$  for isothermal electron species,  $\gamma_e = 5/3$  for non-relativistically degenerate electron species, and  $\gamma_e = 4/3$  for ultra-relativistically degenerate electron species, which are of our present interest. It is important to mention here that the 2nd term ( $\nu \phi^{(1)}/2\tau$ ) in (25) is due to the effect of the nonplanar geometry, and that for  $\nu = 0$  or  $\tau \rightarrow \infty$ , the effect of the nonplanar geometry disappears, and turns to be the 1D planar geometry.

### 1. 1D Planar geometry ( $\nu = 0$ )

We first consider planar geometry by substituting  $\nu = 0$  or  $\tau \rightarrow \infty$  into (25). The assumption  $\nu = 0$  or  $\tau \rightarrow \infty$  reduces (25) to a standard K-dV equation. To obtain the stationary solitary wave (SW) solution of the standard K-dV equation or (25) with  $\nu = 0$ , we consider a moving frame  $\zeta = \xi - \mathcal{U}_0 \tau$ , where  $\mathcal{U}_0$  is the SW speed in the moving frame, and impose the appropriate boundary conditions, viz.  $\phi^{(1)} \rightarrow 0$  and  $d\phi^{(1)}/d\zeta \rightarrow 0$  at  $\zeta \rightarrow \pm\infty$ .

Thus, the stationary SW solution of (25) with  $\nu = 0$  is given by

$$\phi^{(1)} = \psi \operatorname{sech}^2 \left( \frac{\zeta}{\delta} \right), \quad (28)$$

where  $\psi$  and  $\delta$ , respectively, represent the amplitude and the width of the TDPD NA SWs, since (28) represents the TDPD NA SWs with the positive electrostatic wave potential, corresponding to the density compression (in the form of the solitary profile) of the light nucleus species. This is because of  $\mathcal{A} > 0$  and  $\mathcal{B} > 0$ . The amplitude ( $\psi$ ) and the width ( $\delta$ ) of the TDPD NA SWs are, respectively, given by

$$\psi = \frac{3\mathcal{U}_0}{\mathcal{A}}, \quad (29)$$

$$\delta = \sqrt{\frac{4\mathcal{B}}{\mathcal{U}_0}}. \quad (30)$$

It is obvious from (29) and (30) that the amplitude (width) of the TDPD NA SWs directly (inversely) proportional to  $\mathcal{U}_0$  (i.e.  $\psi \propto \mathcal{U}_0$  and  $\delta \propto 1/\mathcal{U}_0$ ).

We now graphically show how the basic features, viz. speed  $\mathcal{M}$ , amplitude  $\psi$ , and width  $\delta$  of the TDPD NA SWs vary with typical plasma parameters, viz.  $\mu$ ,  $\gamma_e$ ,  $\sigma_l$  and  $\beta$  corresponding not only to hot white dwarfs [26–30], but also to many space plasma environments, where non-degenerate electron-ion plasma with heavy positively charged particles (as impurity or dust) occur [34–36]. The results are displayed in figures 1–3, and are interpreted in discussion section. It is important to mention here that for completely non-degenerate plasma system (containing isothermal electron species, non-degenerate warm ion species, and positively charged stationary heavy particles as impurity or dust species),  $\gamma_e = 1$  and  $\beta = 0$  (shown in the solid curve in the left panel of figure 1, whereas in both left and right panel of figure 2, and that these solid curves correspond to the space plasma environments like mesosphere [34–36].

### 2. Non-planar geometry ( $\nu \neq 0$ )

We are now interested in direct numerical solutions of (25) to observe the time evolution of the TDPD NA cylindrical ( $\nu = 1$ ) and spherical ( $\nu = 2$ ) SWs in the TDP systems under consideration. The initial pulse that we have used in our numerical analysis is (28) which valid for  $\tau \rightarrow \pm\infty$ . To mean ‘time from past to present’, we use  $\tau < 0$ . Thus, the initial pulse for the numerical solutions of (25) can be expressed as

$$\phi^{(1)}(\tau \rightarrow \pm\infty) = \psi \operatorname{sech}^2 \left( \frac{\zeta}{\delta} \right). \quad (31)$$

We note that for a large value of  $\tau$ , the TDPD NA solitary profiles represented by (28) are identical to those represented by (31), since the effects of nonplanar geometry represented by the term  $\nu \phi^{(1)}/2\tau$  disappear for the

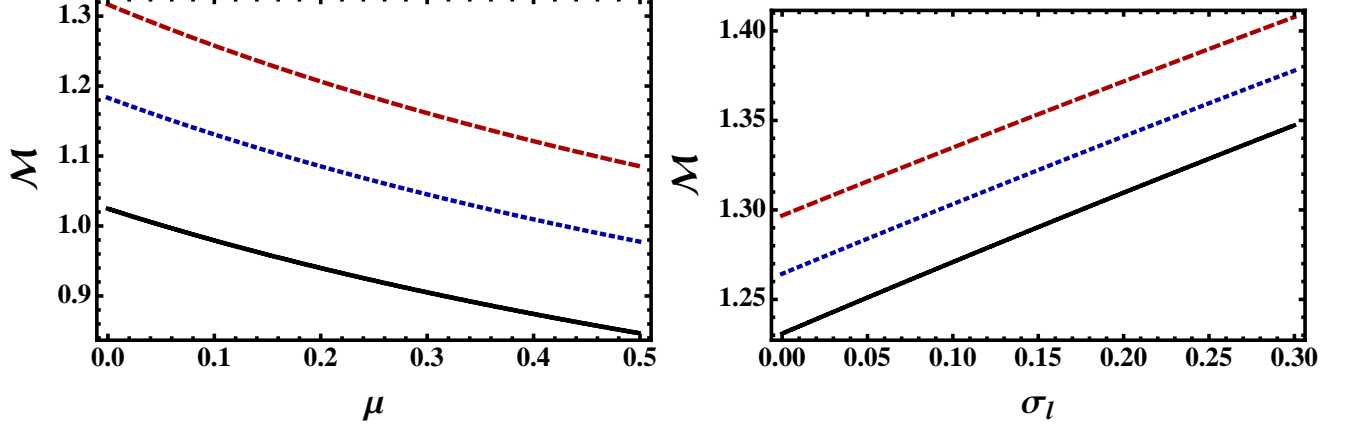


FIG. 1: The variation of the normalized TDPD NA wave phase speed  $\mathcal{M}$  with  $\mu$  for  $\sigma_l = 0.05$ ,  $\{\beta = 0.0, \gamma_e = 1\}$  (solid curve),  $\{\beta = 0.01, \gamma_e = 4/3\}$  (dotted curve) and  $\{\beta = 0.01, \gamma_e = 5/3\}$  (dashed curve) in the left panel, whereas that with  $\sigma_l$  for  $\gamma_e = 5/3$ ,  $\mu = 0.1$ ,  $\beta = 0$  (solid curve),  $\beta = 0.05$  (dotted curve) and  $\beta = 0.1$  (dashed curve) in the right panel.

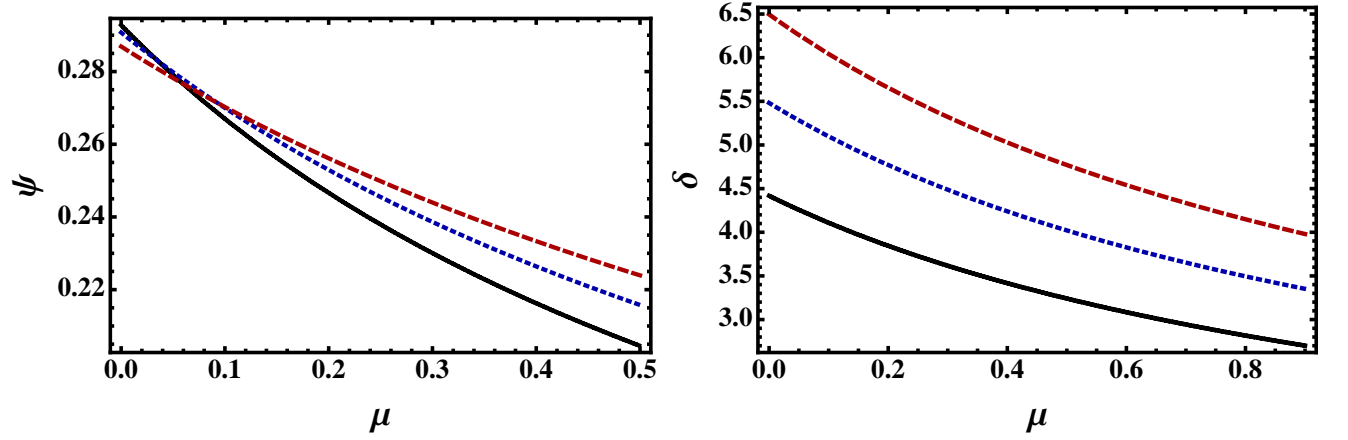


FIG. 2: The variation of the normalized TDPD NA SW amplitude  $\psi$  (left panel) and width  $\delta$  (right panel) with  $\mu$  for  $\sigma_l = 0.05$ ,  $\mathcal{U}_0 = 0.1$ ,  $\{\beta = 0.0, \gamma_e = 1\}$  (solid curve),  $\{\beta = 0.01, \gamma_e = 4/3\}$  (dashed curve).

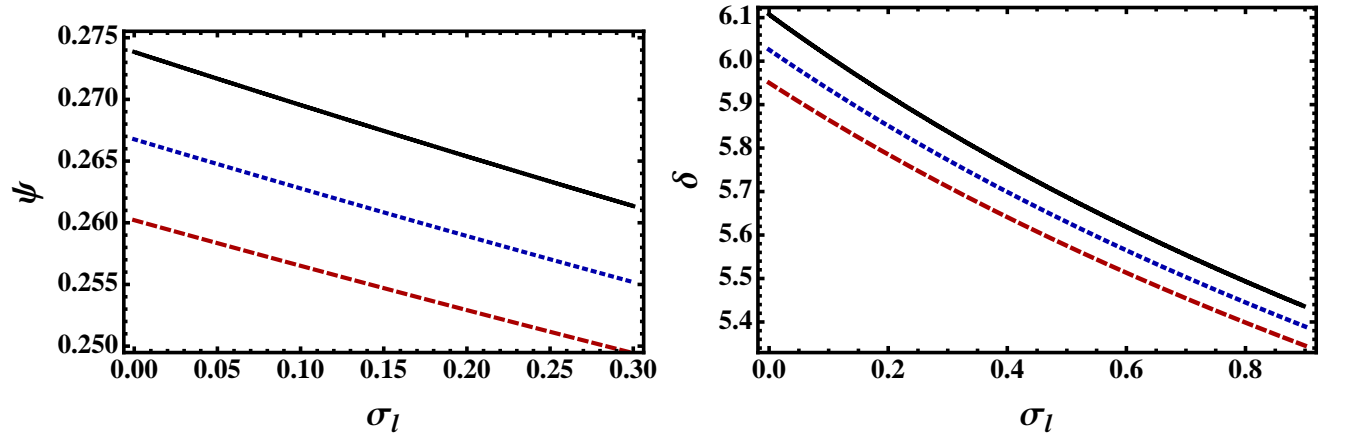


FIG. 3: The variation of the normalized TDPD NA SW amplitude  $\psi$  (left panel) and width  $\delta$  (right panel) with  $\sigma_l$  for  $\mu = 0.1$ ,  $\gamma_e = 5/3$ ,  $\mathcal{U}_0 = 0.1$ ,  $\beta = 0$  (solid curve),  $\beta = 0.05$  (dotted curve), and  $\beta = 0.1$  (dashed curve).

large value of  $\tau$ . We have obtained the direct numerical solutions of (25) using this initial pulse, and using typical plasma parameters corresponding to hot white dwarfs [26–30]. The direct numerical solutions of (25) is displayed in figure 4.

We have also found the direct numerical solutions of (25) using the initial pulse represented by (31), and using typical plasma parameters corresponding to space plasma environments like mesospheres, where  $\gamma_e = 1$  and  $\beta = 0$  [34–36]. The direct numerical solutions of (25) is displayed in figure 5.

The direct numerical solutions of (25), which have been displayed in figures 4 and 5, clearly indicate that for a large value of  $\tau$  (e.g.  $\tau = -16$ ) the spherical and cylindrical TDPD NA SWs are similar to the 1D planar ones. This is because that the time and geometry dependent extra term  $(\nu/2\tau)\phi^{(1)}$  in (25) has become insignificant. However, as the value of  $\tau$  decreases, the term  $(\nu/2\tau)\phi^{(1)}$  becomes significant, and both the spherical and cylindrical SWs differ from the 1D planar ones.

#### IV. DISCUSSION

The novel TDP model (based on the plasma system containing thermally degenerate electron species, thermally degenerate light nucleus species, and low dense stationary heavy nucleus species) has been considered to study the TDPD NA SWs in 1D planar as well as in cylindrical and spherical nonplanar geometries. The basic features of these TDPD NA SWs in such a plasma system have been investigated by the reductive perturbation method [31–33], which is valid for small but finite amplitude TDPD NA SWs. The results, which have been observed from this theoretical and numerical investigations, can be summarized as follows:

1. The presence of stationary heavy nucleus species in electron-nucleus plasma supports the existence of subsonic TDPD NA SWs with  $\phi > 0$  in both planar and nonplanar geometries. The increase in number density of stationary heavy nucleus species increases (decreases), but that in thermal and degenerate pressures of the TDP species decreases (increases) the possibility for the formation of the subsonic (supersonic) TDPD NA SWs. This is due to the fact that the phase speed of the TDPD NA waves decreases (increases) with the rise of the number density of the stationary heavy nucleus species (thermal and degenerate pressures of the TDP species).
2. The amplitude (width) of the TDPD NA SWs increases (decreases) with the rise of the number density of the heavy nucleus species in both planar and nonplanar geometries. This is because of the decrease in the TDPD NA wave phase speed with the rise of the stationary heavy nucleus number density.

3. The amplitude (width) of the TDPD NA SWs decreases (increases) with the rise of the light nucleus thermal pressure in both planar and nonplanar geometries. This is due to the fact that thermal pressure of the light nucleus fluid enhances the random motion of the light nucleus species, which causes to decrease (increase) the amplitude (width) of the TDPD NA solitary structures in any geometry under consideration.
4. The amplitude of the TDPD NA SWs for ultra-relativistically degenerate electron species is smaller than that for non-relativistically degenerate electron species, but is larger than that for isothermal electron species. On other hand, their width for non-relativistically degenerate electron species is larger than that for ultra-relativistically degenerate electron species, but is smaller than that for isothermal electron species in both planar and nonplanar geometries. This is due to that fact that the amplitude (width) of the SWs increases (decreases) as the value of  $\gamma_e$  increases.
5. The amplitude of cylindrical and spherical TDPD NA SWs increases as the value of  $\tau$  decreases for both degenerate and non-degenerate plasmas. The amplitude of cylindrical TDPD NA SWs is larger than that of 1D planar ones, but smaller than that of the spherical ones. This is due to the time and geometry dependent extra term  $(\nu/2\tau)\phi^{(1)}$  in the MK-dV equation.

There are many hot white dwarfs [26–30], where the electron thermal pressure can be comparable to or greater than its degenerate pressure, and where in addition to non or ultra-relativistically degenerate electron species [2–4, 6] and non-relativistically degenerate light nucleus species (viz.  ${}^1_1\text{H}$  [2, 4], or  ${}^4_2\text{He}$  [6] or  ${}^{12}_6\text{C}$  [7], the stationary heavy nucleus species (viz.  ${}^{56}_{26}\text{Fe}$  [11] or  ${}^{85}_{37}\text{Rb}$  [12] or  ${}^{96}_{42}\text{Mo}$  [12]) exists.

On the other hand, non-degenerate electron species [defined by (9) as a special case of  $\gamma_e = 1$ ], ions [identical to light nucleus species], and positively charged particle (impurity/dust species [identical to stationary heavy nucleus species] are observed in many space plasma environments [34–36].

The novel TDP model under our present consideration is so general that it is applicable not only in astrophysical compact objects like hot white dwarfs [26–30], but also in many space environments like mesospheres [34–36] containing positively charged heavy stationary particles (as impurities or dust) in addition to isothermal electron and warm ion plasma species.

The mesospheric plasma parameters corresponds to  $\gamma_e = 1$ ,  $\beta = 0$ ,  $\mu = 0.1 - 0.3$ , and  $\sigma_l = 0.01 - 0.1$ . The basic features of the subsonic and supersonic SWs are displayed in solid curves in left panel of figure 1 and in both left and right panels of figure 2 for 1D planar geometry, and in all cures in figure 5 for cylindrical (left panel) and spherical (right panel) geometries.

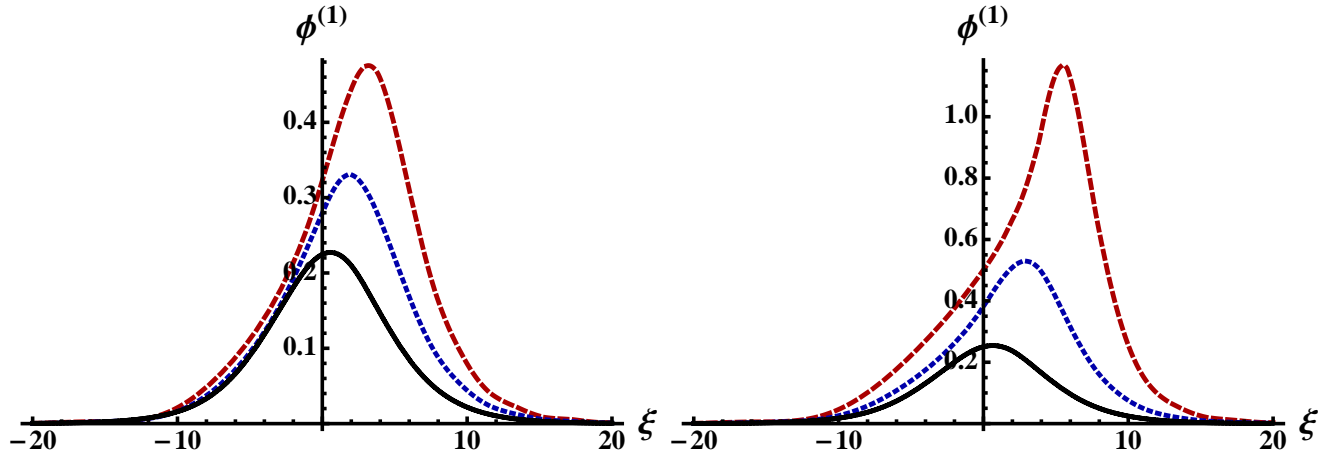


FIG. 4: The effects of cylindrical (left panel) and spherical (right panel) geometries on the SWs associated with the TDPD NA wave potential for  $\mathcal{U}_0 = 0.1$ ,  $\mu = 0.3$ ,  $\sigma_l = 0.1$ ,  $\gamma_e = 5/3$ ,  $\beta = 0.05$ ,  $\tau = -16$  (solid curves),  $\tau = -8$  (dotted curves) and  $\tau = -4$  (dashed curve).

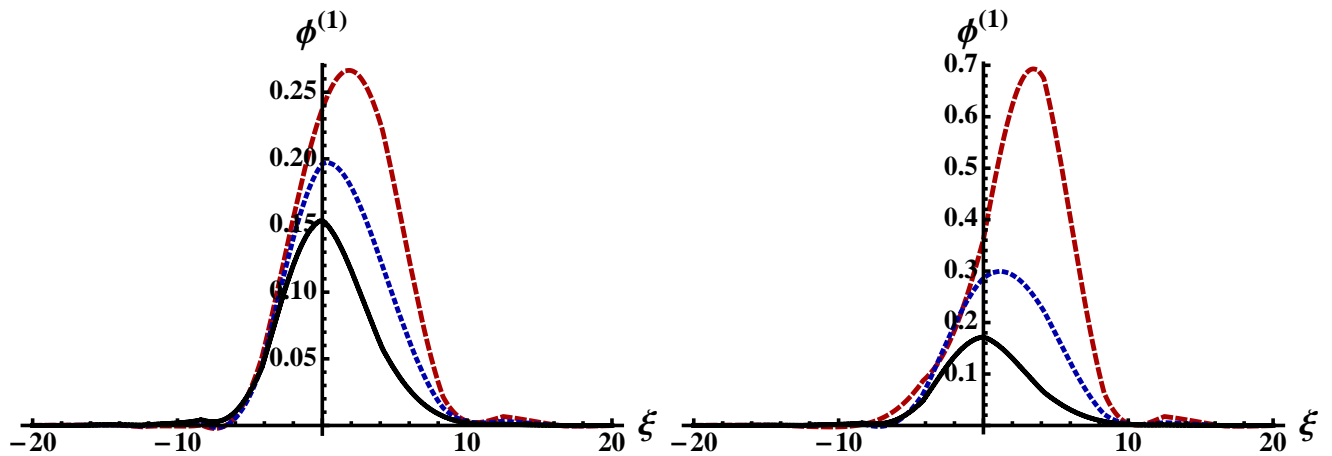


FIG. 5: The effects of cylindrical (left panel) and spherical (right panel) geometries on the SWs associated with the TDPD NA wave potential for  $\mathcal{U}_0 = 0.1$ ,  $\mu = 0.3$ ,  $\sigma_l = 0.1$ ,  $\gamma_e = 1$ ,  $\beta = 0$ ,  $\tau = -16$  (solid curves),  $\tau = -8$  (dotted curves) and  $\tau = -4$  (dashed curve).

The limitation of the reductive perturbation method used here is that it is not valid for arbitrary or large amplitude TDPD NA SWs. To overcome this limitation, we have to develop a correct numerical code, and to solve (10)–(12) with (9) numerically by the numerical code to be developed. This type of numerical analysis will be able to show the time evolution of large amplitude TDPD NA SWs. This is a challenging research problem of great importance, but beyond the scope of our present work.

However, we hope that our present work will be helpful to understand the physics of localized electrostatic disturbances in astrophysical compact objects like hot white dwarfs, e.g. DQ white dwarfs [26, 27, 30], white dwarf H1504+65 [28], and white dwarf PG 0948+534 [29]. We also expect that our present work will also be useful for understanding the physics of localized electrostatic disturbances in many space environments, e.g. mesosphere [34–36].

---

[1] FOWLER, R. H. 1926 On Dense Matter. *MNRAS* **87**, 114–122.

[2] CHANDRASEKHAR, S. 1931 The Density of White Dwarf Stars. *Phil. Mag.* **11**, 70.

- [3] CHANDRASEKHAR S. 1931 The Maximum Mass of Ideal White Dwarfs. *Astrophys. J.* **74**, 81-82.
- [4] CHANDRASEKHAR, S. 1936 The pressure in the interior of a star. *NRAS* **96**, 644-647.
- [5] KOESTER, D. & CHANMUGAM, G. 1990 Physics of white dwarf stars. *Rep. Prog. Phys* **53**, 837-916.
- [6] HORN, H. M. V. 1991 Dense astrophysical plasmas. *Science* **252**, 384-389.
- [7] KOESTER, D. 2002 White dwarfs: Recent developments. *Astron. Astrophys. Rev.* **11**, 3366.
- [8] SHUKLA, P. K. AND ELIASSON, B. 2011 Nonlinear collective interactions in quantum plasmas with degenerate electron fluids. *Rev. Mod. Phys.* **83**, 885-906.
- [9] SHUKLA, P. K., MAMUN, A. A. & MENDIS, D. A. 2011 Nonlinear ion modes in a dense plasma with strongly coupled ions and degenerate electron fluids. *Phys. Rev. E* **84**, 026405.
- [10] BRODIN, G, EKMAN, R. & ZAMANIAN J. 2016 Quantum kinetic theories in degenerate plasmas. *Plasma Phys. Control. Fusion* **59**, 014043.
- [11] VANDERBURG, A. J., JOHNSON, A., RAPPAPORT, S., BIERLYA, A., IRWIN, J., LEWIS, J. A., KIPPING, D., BROWN, D. R., DUFOUR, P., CIARDI D. R. *et al.* 2015 A disintegrating minor planet transiting a white dwarf. *Nature* **526**, 546549.
- [12] WITZE, A. 2014 Space-station science ramps up. *Nature* **510**, 196.
- [13] TONKS, L. & LANGMUIR, I. 1929 Oscillations in Ionized Gases. *Phy. Rev.* **33**, 195-210.
- [14] REVANS, R. W. 1933 The transmission of waves through an ionized gas. *Phy. Rev.* **44** 798-902.
- [15] MAMUN, A. A. 2018 Degenerate pressure driven modified nucleus-acoustic waves in degenerate plasmas. *Phys. Plasmas* **25**, 024502.
- [16] MAMUN, A. A., AMINA, M. & SCHLICKEISER, R. 2016 Nucleus-acoustic shock structures in a strongly coupled self-gravitating degenerate quantum plasma. *Phys. Plasmas* **23**, 094503.
- [17] MAMUN, A. A., AMINA, M. & SCHLICKEISER, R. 2017 Heavy nucleus-acoustic spherical solitons in self-gravitating super-dense plasmas. *Phys. Plasmas* **24**, 042307.
- [18] ZAMAN, D. M. S., AMINA, M., DIP, P. R. & MAMUN, A. A. 2017 Planar and nonplanar nucleus-acoustic shock structures in self-gravitating degenerate quantum plasma systems. *Euro Phys J. Plus* **132**, 457.
- [19] ZAMAN, D. M. S., AMINA, M., DIP, P. R. & MAMUN, A. A. 2018 Nucleus-acoustic solitary waves in self-gravitating degenerate quantum plasmas. *Chinese Phys. B* **27**, 040402.
- [20] JANNAT, S. & MAMUN, A. A. 2018 Nucleus-acoustic shock waves in white dwarfs. *Pramana - J. Phys.* **90**, 51.
- [21] JANNAT, S. & MAMUN, A. A. 2018 Nucleus-acoustic solitary waves in white dwarfs. *Chinese J. Phys.* **56**, 3046-3052.
- [22] SULTANA, S. & SCHLICKEISER, R. 2018 Arbitrary amplitude nucleus-acoustic solitons in multi-ion quantum plasmas with relativistically degenerate electrons. *Phys. Plasmas* **25**, 022110.
- [23] SULTANA, S., ISLAM, S., MAMUN, A. A. & SCHLICKEISER, R. 2018 Modulated heavy nucleus-acoustic waves and associated rogue waves in a degenerate relativistic quantum plasma system. *Phys. Plasmas* **25**, 012113.
- [24] CHOWDHURY, N., A., HASAN, M. M. MANNAN, A. & MAMUN, A. A. 2018 Nucleus-acoustic envelope solitons and their modulational instability in a degenerate quantum plasma system. *Vacuum* **147**, 31-37.
- [25] DAS P. & KARMAKAR, P. K. 2019 Nonlinear nucleus-acoustic waves in strongly coupled degenerate quantum plasmas. *Europhys. Lett.* **126**, 10001.
- [26] DUFOUR, P., FONTAINE, G., LIEBERT, J., SCHMIDT, G. D. & BEHARA, N. 2008 Hot DQ white dwarfs: something different. *Astrophys. J.* **683**, 978-989.
- [27] DUFOUR, P., BÉLAND, S., FONTAINE, G., CHAYER, P. & BERGERON, P. 2011 Taking advantage of the COS time-tag capability: Observations of pulsating Hot DQ white dwarfs and discovery of a new one. *Astrophys. J. Lett.* **733**, L19.
- [28] WERNER, K. & RAUCH, T. 2015 Analysis of HST/COS spectra of the bare CO stellar core H1504+65 and a high-velocity twin in the Galactic halo. *Astron. Astrophys.* **584**, A19.
- [29] WERNER, K., RAUCH, R. & REINDL, N. 2019 Spectral analysis of the extremely hot DA white dwarf PG 0948 + 534. *MNRAS* **483**, 52915300.
- [30] KOESTER, D., KEPLER, S. O. & IRWIN, A. W. 2020 New white dwarf envelope models and diffusion-Application to DQ white dwarfs. *Astron. Astrophys.* **635**, A103.
- [31] WASHIMI H. & TANIUTI, T. 1966 Propagation of ion-acoustic solitary waves of small amplitude. *Phys. Rev. Lett.* **17**, 996-997.
- [32] MAXON, S. & VIECELLI, J. 1974 Spherical Solitons. *Phys. Rev. Lett.* **32**, 4-5.
- [33] MAMUN, A. A. & SHUKLA, P. K. 2002 Cylindrical and spherical dust ion-acoustic solitary waves. *Phys. Plasmas* **9**, 1468-1470.
- [34] HAVNES O., TRØIM, J., BLIX, T., MORTENSEN, W., NÆSHEIM, L. I., THRANE, E. & TØNNESSEN, T. 1996 First detection of charged dust particles in the Earth's mesosphere. *J. Geophys. Res.* **101**, 10839-10847.
- [35] GELINAS, L. J., LYNCH, K. A., KELLEY, M. C., COLLINS, S., BAKER, S., ZHOU Q. & FRIEDMAN, . S. J. 1998 First observation of meteoritic charged dust in the tropical mesosphere. *Geophys. Res. Lett.* **25**, 4047-4050.
- [36] MENDIS, D, A., WONG, WAI-HO, AND ROSENBERG, M. 2004 On the observation of charged dust in the tropical mesosphere. *Phys. Scripta* **T113**, 141-143.